



SEISMIC PERFORMANCE OF MASONRY INFILLED R/C FRAMES

Luis DECANINI¹, Fabrizio MOLLAIOLI¹, Andrea MURA¹, Rodolfo SARAGONI²,

SUMMARY

It is well known that masonry infills, although non-engineered and considered as non-structural, may provide most of the earthquake resistance and prevent collapse of relatively flexible and weak RC structures. The objective of this study is to investigate the effect of masonry infills on the performance of reinforced concrete frames subjected to earthquake ground motions. To this purpose an equivalent discrete shear-type model with and without infills was used for the evaluation of elastic and inelastic response of multi-story frame structures. The masonry-infilled modeled by means of equivalent strut elements, which can only carry compressive loads, characterized by an idealized degrading hysteretic behavior. The adopted mathematical models was validated by comparing numerical and test results. To investigate the influence of the mechanical characteristics of the infills, three different idealized type of masonry infills were considered, defined as weak, intermediate and strong. The performance of a large number of different reinforced concrete two bay-frames, bare and infilled, subjected to ten ground motion was investigated. The wide range of natural periods taken into account allowed to establish response spectra for several significant parameters characterizing the behavior of bare and infilled frames. The results of the investigation suggest that the global non-linear seismic response of reinforced concrete frames with masonry infill can be simulated by a relatively simple mathematical model, which combines a shear-type model with equivalent strut elements representing the infill walls, provided that the infill does not fail out of plane. Moreover, infills, if present in all storeys, give a significant contribution to the energy dissipation capacity, reducing the dissipation energy demands in frame elements and decreasing significantly the maximum displacements. Therefore the contribution of masonry is of great importance, even though strongly depending on the characteristics of the ground motion, especially for non-seismic frames, which have a lower capacity of dissipating energy than the seismic ones.

INTRODUCTION

The observation of the response of building structures, engineered or not engineered to resist major or moderate earthquakes, after the past earthquakes highlighted the significant contribution of the infills in the characterization of their seismic behavior. Infills were usually classified as non structural elements, and their influence was neglected during the modeling phase of the structure leading to substantial inaccuracy in predicting the actual seismic response of framed structures. From the point of view of

¹ University of Rome "La Sapienza", Italy

² University of Chile, Chile

structural response, the infilled frames presents a wide variability due to the characteristics of the ground motion, the mechanical properties of infills, the overall geometry, the frame-to-infill interface behavior, the horizontal or vertical arrangement of the infills, the presence of openings and their dimension and location, etc. Moreover, the problem of the out-of-plane behavior of infilled frames deserves appropriate attention not only because its potentially dangerous effect, but also in terms of its interaction with in-plane response. The impact of the infills on the seismic behavior of buildings may be positive or negative, depending on a large number of influential parameters. Generally, the performance of the structure can be significantly improved by the increase of strength and dissipation capacity due to the masonry infills, even if in presence of an increasing in earthquake inertia forces. However, for a proper design of masonry infilled reinforced concrete frames it is necessary to completely understand their behavior under repeated horizontal loading. Neglecting the significant interaction between the filler walls and building frames is the main reason why structural systems incorporating integrated infills panels react to strong earthquakes in a manner quite different from the expected one.

Another important issue is related to the numerical simulation of infilled frames. The different techniques for idealizing this structural model can be divided into two local or micro-models and simplified macro-models (Crisafulli [1], Shing [2]). The first group involves the models, in which the structure is divided into numerous elements to take into account of the local effect in detail, whereas the second group includes simplified models (Klingner [3], Bertero [4], Decanini [5], Kappos [6], Fardis [7]) based on a physical understanding of the behaviour of the infill panel. In this paper the infill panels were modeled by equivalent diagonal struts, which carry loads only in compression. Three different type of masonry were considered, namely weak, intermediate, and strong infills, whose mechanical properties, derived from experimental tests, are function of the characteristics of both the frame and the infill panel, and consequently takes into account their interaction. The diagonal strut model, representing the infill panels were therefore implemented in an equivalent discrete shear-type model, that allowed to perform a large number of dynamic analyses on a set of reinforced concrete two-bay bare and infilled frames subjected to earthquake ground motions, in order to establish response spectra of the most significant parameters characterizing the behavior of multi-degree-of-freedom systems.

MODELING OF INFILLED FRAMES AND GROUND MOTIONS

In this paper, for modelling MDOF systems a simplified equivalent discrete shear-type model, namely ESTM model, whose lateral stiffness, inertial and strength characteristics approximate those of the frame structure and can vary along the height, was adopted (Decanini [8]). This choice provided a relatively easy numerical procedure that permitted to extend the analyses to a wide range of signals and structures and to establish response spectra also for aspects of the seismic demand that cannot be studied by means of SDOF systems, such as the inter-story drift and story energy dissipation demand. With this model, the contribution of all the vibration modes of the structure can be implicitly considered for the evaluation of the inelastic response, and the distribution of displacement and energy dissipation on the height of the structure can be adequately described. Moreover, the structural system can be completely described by the stiffness and mass properties of the stories.

For the prediction of the inelastic response of a frame structure subjected to a ground motion, a further approximation was introduced in order to describe the hysteretic behavior of the system by means of simple rules. As for the story stiffness, also a story yielding resistance can be approximately defined. Even though it implies to neglect some information on local inelastic deformations and hysteretic dissipations, as plastic curvature and dissipated energy in portions of members, on the other hand it allows to conduct a wide investigation into the inelastic seismic response of multi-story buildings.

In this research, ten different R/C two bay-frames (Figure 1), having constant story height and beam spans, with ten different numbers ($N=2, 4, 6, 8, 10, 12, 14, 16, 20, 24$) of stories were selected in order to assume information on the seismic response of a wide range of current buildings.

A stiffness-degrading hysteretic model was adopted for the cyclic behavior of the bare frames in each story. The hysteresis model used in this study utilizes several control parameters that establish the rules for inelastic loading reversals. Stiffness degradation is modeled as a function of ductility; strength deterioration is modeled as a function of both dissipated energy and ductility; and pinching is modeled by two independent parameters to control the degree of pinching. The yielding strengths of the stories were obtained by an inverted-triangular distribution of equivalent seismic forces, with an additional force at the top of the building with fundamental periods over 0.7 s. The analyses were performed for four different values of the base shear seismic coefficient C_y of the bare frame, namely 0.15, 0.20, 0.30, and 0.40. Rayleigh damping was used to obtain a 5% of critical damping in the first and in the second modes.

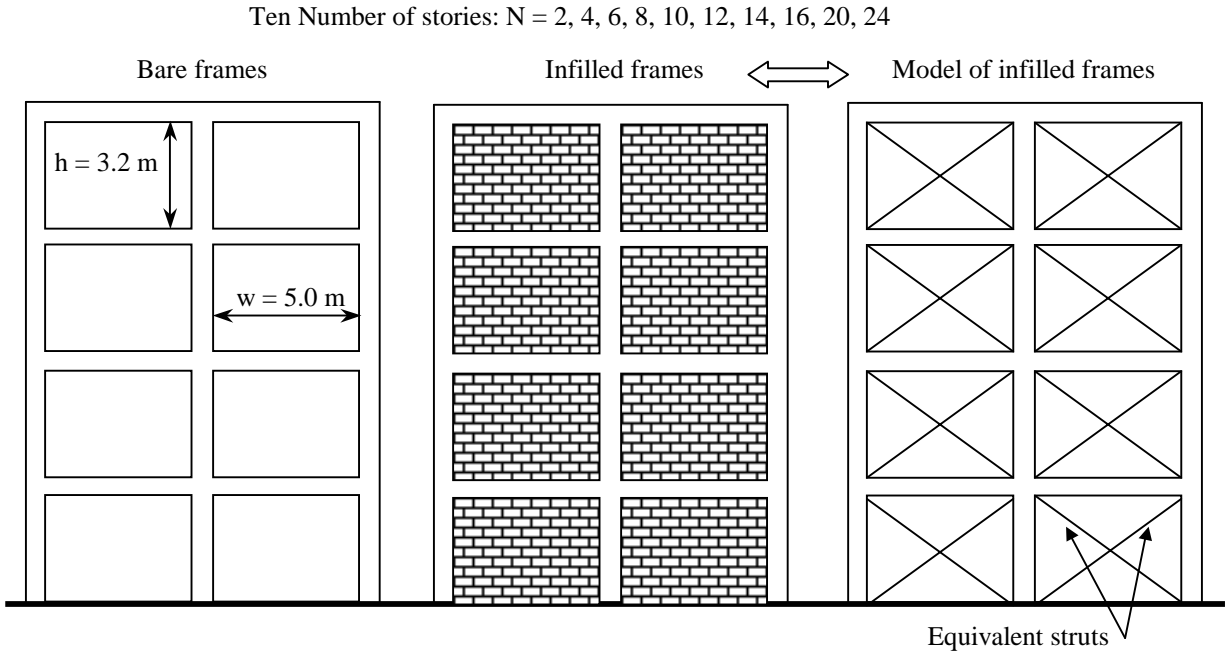


Figure 1. Structural layout of the bare and infilled frames.

Modeling of infills

The adopted model assumes that the contribution of the masonry infill panel to the response of the infilled frame can be modeled by replacing the panel by a system of two diagonal masonry compression struts. The individual masonry struts are considered to be ineffective in tension. However, the combination of both diagonal struts provides a lateral load resisting mechanism for positive as well as negative direction of loading. On the basis of test results a phenomenological hysteresis model for the masonry infill was proposed by Decanini [5, 9, 10]. The adopted modeling was originally intended for use by considering monotonic lateral loads. Nevertheless, in calibrating and assessing the stiffness and strength of the equivalent strut, the reversible cyclical nature of the seismic loads was taken into account. As described in Figure 2 the skeleton curve of the lateral force-displacement (H_m-u) relationship consider four branches. The first linear elastic ascending branch corresponds to the uncracked stage, the second branch refers to the post-cracking phase up to the development of the maximum strength (H_{mfc}). The point FC corresponds to the complete cracking stage of the infill panel. The descending third branch of the curve describes the post-peak strength deterioration of the infill up to reach the residual strength and displacement H_{mr} and u_r , respectively; after that the curve continues horizontally. The model needs essentially of the definition of the width of the equivalent strut ω , the stiffness at complete cracking stage K_{mfc} , and the strength H_{mfc} , as a function of the geometric and mechanical characteristics of the frame.

The width of the strut ω is introduced by means of the relative stiffness parameter λh proposed by Stafford-Smith [11] and by two constants K_1 and K_2 calibrated on the basis of experimental tests:

$$\omega = \left(\frac{K_1}{\lambda h} + K_2 \right) d \quad (1)$$

where λh is a non-dimensional parameter depending on the geometric and mechanical characteristics of the frame-infill system, K_1 and K_2 are coefficients that change according to λh , and d is the length of the equivalent strut.

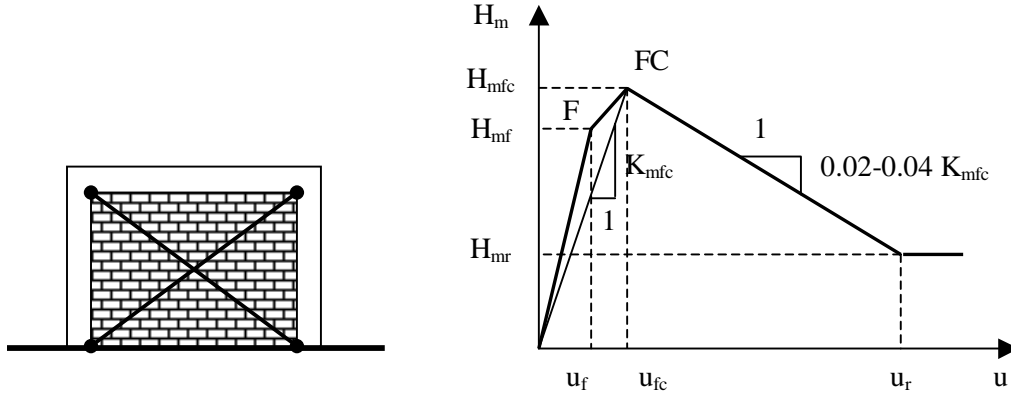


Figure 2. Force-displacement envelope curve of the equivalent strut.

It is well known that the parameter λh , originally proposed by Stafford-Smith [11], is defined by the following expression:

$$\lambda h = 4 \sqrt{\frac{E_m e \sin(2\theta)}{4E_c I h_m}} h \quad (2)$$

where E_m is the elastic equivalent modulus corresponding to the complete cracking stage of the infill, E_c is the elastic modulus of concrete, t is the slope of the strut to the respect of the horizontal axis, e is the thickness of the masonry panel, h is the story height, h_m is the height of the masonry panel, I is momentum of inertia of the columns.

The stiffness of the equivalent strut K_{mfc} at complete cracking stage is given by the following relation:

$$K_{mfc} = \frac{E_m e \omega}{d} \cos^2 \theta \quad (3)$$

The resistance of the infill panel was simulated by a fictitious failure compressive stress σ_{br} , taking the different failure modes occurred in both conventional tests and real structures subjected to seismic action into account. Four basic failure modes are considered, with the corresponding equivalent failure compressive stresses: (a) diagonal tension, $\sigma_{br(1)}$; (b) sliding shear along horizontal joints, $\sigma_{br(2)}$; (c) crushing in the corners in contact with the frame, $\sigma_{br(3)}$; (d) diagonal compression, $\sigma_{br(4)}$.

$$\sigma_{br(1)} = \frac{0.6 \tau_{m0} + 0.3 \sigma_o}{\omega / d} \quad (4)$$

$$\sigma_{br(2)} = \frac{(1.2 \sin \theta + 0.45 \cos \theta) f_{sr} + 0.3 \sigma_o}{\omega / d} \quad (5)$$

$$\sigma_{br(3)} = \frac{(1.12 \sin \theta \cos \theta)}{K_1 (\lambda h)^{-0.12} + K_2 (\lambda h)^{0.88}} \sigma_{m0} \quad (6)$$

$$\sigma_{br(4)} = \frac{1.16 \sigma_{m0} \tan \theta}{K_1 + K_2 \lambda h} \quad (7)$$

where σ_{m0} is the vertical compression strength measured on masonry specimens, τ_{m0} is the shear strength measured with the diagonal compression test, f_{sr} is the slide resistance in the joints measured from the triplet test, and σ_0 is the vertical stress due to working loads.

Once determined the fictitious failure compressive stresses corresponding to the different failure modes, the minimum value ($\sigma_{br})_{min}$ defines the most probable mode of failure, the lateral strength of the equivalent strut is given by:

$$H_{mfc} = (\sigma_{br})_{min} e \omega \cos \theta \quad (8)$$

The original model, based on an equivalent strut approach for masonry infill panels to be used in non-linear analysis of building structures, was updated to include (Mura [12]) hysteretic effects characteristics of structural masonry elements subjected to repeated loading reversals such as stiffness degradation, strength deterioration and pinching. The model was implemented to replicate a wide range of hysteretic force-displacement behavior resulting from different design and geometry by varying the control parameters of the model.

In the present research, three different type of masonry, whose properties are reported in Table 1, classified as weak infills (t1), intermediate infills (t2), and strong infills (t3), as already selected by Liberatore [13] on the basis of comparison with experimental tests, were utilized in the analyses.

Table 1. Masonry infills description and mechanical characteristics.

| Infills type | Bricks | Mortar | Masonry | | |
|-------------------|---|---------------------|---------------------|-------------------|-------------|
| | | | σ_{m0} (MPa) | τ_{m0} (MPa) | E_m (MPa) |
| Weak (t1) | Hollow bricks thickness 120 mm | Cement +sand + lime | 1.20 | 0.20 | 1050 |
| Intermediate (t2) | Hollow bricks thickness 145 mm | Cement +sand | 2.10 | 0.40 | 1880 |
| Strong (t3) | Semi-solid bricks UNI thickness 120 mm | Cement +sand | 11.50 | 0.84 | 6000 |

σ_m =compressive strength (MPa), τ_{m0} =shear strength, evaluated through diagonal compressive test (MPa), E_m =initial elastic modulus (MPa)

Moreover, the model was validated and verified by comparing the calculated and measured response of several specimens (Parducci [14, 15], Stylianidis [16], Pires [17]). Comparing the experimentally obtained results with the analytically obtained ones, it was verified that the proposed model could reasonably used for the estimation of the seismic response of infilled frame structures. Even though several comparisons were made, for the sake of brevity herein only two were illustrated.

The first comparison is related to the cyclic experimental test, at imposed displacements, performed by Pires [17] on bare and infilled one-bay frames. The displacement time history of the reported comparison (model M2) was constituted by 38 half-cycle with increasing amplitude up to ± 100 mm. The infilled masonry was realized with hollow bricks (30x20x15 cm) having mechanical properties analogous to the t2 type (intermediate). In Figure 3 the base shear vs. horizontal displacement cyclic response obtained by means of the ESTM model is illustrated. Maximum (F_{max}) and minimum (F_{min}) force values and that corresponding to the last half-cycle (F_{37} and F_{38}), and are also indicated in Table 2. It is possible to note that the numerical analyses provide on average a slight underestimation of the experimental values in

terms of forces. Moreover, the energy dissipated during the numerical test is about 10-12 % less than that dissipated during the experimental tests, confirming that the ESTM model correctly reproduced the cyclic behaviour of the infill frames.

Table 2. Comparison between numerical (ESTM model) and experimental force values. Pires [17] frames.

| | Experimental | Numerical (ESTM) | Numerical/ Experimental |
|----------------|--------------|---------------------|----------------------------|
| F_{max} (kN) | 107 | 102 | 0.95 |
| F_{min} (kN) | -120 | -102 | 0.85 |
| F_{37} (kN) | 58 | 59 | 1.02 |
| F_{38} (kN) | -68 | -61 | 0.90 |

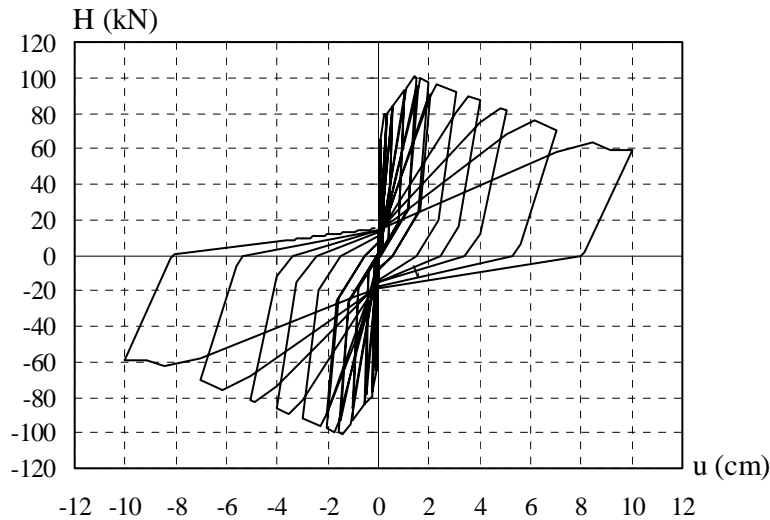


Figure 3. Base shear (H) vs. cyclic horizontal displacement u. Pires [17] M2 frame. ESTM model.

Table 3. Comparison between numerical (ESTM model) and experimental results. Parducci [14, 15] frames.

| N° of cycle | F (kN) | RB3 | | | TB3 | | |
|-------------|-----------|--------------|-----------|----------------------------|--------------|-----------|----------------------------|
| | | Experimental | Numerical | Numerical/ Experimental | Experimental | Numerical | Numerical/ Experimental |
| 1 | F_{max} | 250 | 183 | 0.73 | 240 | 158 | 0.66 |
| | F_{min} | -112 | -160 | 1.43 | -145 | -178 | 1.23 |
| 2 | F_{max} | 63 | 56 | 0.89 | 240 | 67 | 0.28 |
| | F_{min} | -65 | -64 | 0.98 | -90 | -72 | 0.80 |
| 3 | F_{max} | 50 | 46 | 0.92 | 75 | 65 | 0.87 |
| | F_{min} | -50 | -42 | 0.84 | -75 | -63 | 0.84 |
| 4 | F_{max} | 50 | 41 | 0.82 | 50 | 57 | 1.14 |
| | F_{min} | -50 | -39 | 0.78 | -70 | -58 | 0.83 |
| | | | | mean 0.92 | mean 0.83 | | |

A second comparison was carried out on infilled one-bay frames tested by Parducci [14, 15]. Cyclic tests with forced displacements, equal for all cycles to ± 40 mm, were performed on two one-bay frames, RB and TB, having different beam dimensions and column reinforcements. The masonry infill, equal for both frames, was constituted by semi-solid bricks having mechanical characteristics comparable with the strong infills (t3) adopted in the present study. In Table 3 the comparison between experimental tests and numerical analyses for the frames RB3 and TB3 in terms of maximum and minimum base shears (F_{max} and

F_{min}) was reported. It is possible to observe that there is some difference, particularly for the first cycle. In effect the equivalent strut model takes into account the cyclic behaviour by establishing a mean strength for positive and negative loading. As a matter of fact, during a half-cycle some differences may be encountered, that tend to diminish once the whole cycle is considered. This is also confirmed by the fact that there are negligible differences in terms of dissipated cyclic energy. However, the mean ratio between numerical and experimental base shears, equal to 0.92 and 0.83 for the RB3 and TB3 specimen respectively, provided evidence of the quite good conformity of the ESTM model to the experimental tests. Finally, in Figure 4 the cyclic behaviour, in terms of base shear vs. displacement, derived from numerical tests performed with the ESTM model, is shown.

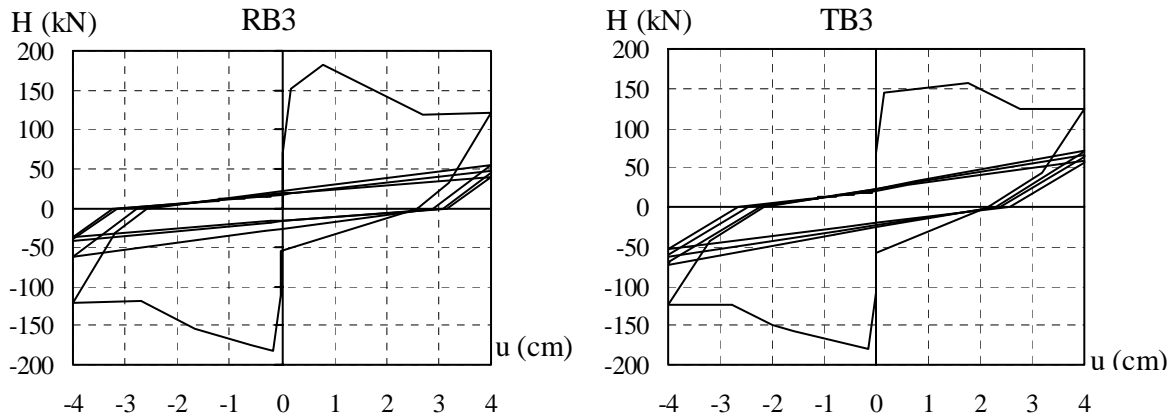


Figure 4. Base shear (H) vs. cyclic horizontal displacement u . Parducci [14, 15] frames. ESTM model.

Ground motions selection

The assessment of demands for bare and infilled frames necessitated the availability of a set of acceleration time histories with amplitude, frequency content, and duration enclosed into certain limits in order to reduce the dispersion of the corresponding demand parameters. Since the frequency content depends on magnitude and distance, the records were selected in narrow magnitude and distance bins. In this paper ten records obtained during earthquakes with moment magnitudes between 6.5 and 7.0 and with different fault mechanisms, at distances (herein the distance from the surface projection of the causative fault, D_f , was adopted) between 10 km and about 20 km, on soil approximately corresponding to a C class according to EC8 [18], were used (Table 4).

Table 4. Earthquakes and records considered.

| Earthquake | Year | M_w | Station | D_f (km) | Name | Comp. |
|------------------|------|-------|------------------------------|------------|----------|-------|
| Montenegro | 1979 | 6.9 | Ulcinj-Hotel Olympic | 10.0 | ULCHOLNS | NS |
| Imperial Valley | 1979 | 6.5 | El Centro Array #2 | 10.2 | KEYSTN14 | N140 |
| Northridge | 1994 | 6.7 | Canyon Country - W Lost Cany | 11.4 | LOS270 | N270 |
| Montenegro | 1979 | 6.9 | Petrovac-Hotel Oliva | 12.0 | PETROVNS | NS |
| Loma Prieta | 1989 | 6.9 | Gilroy Array #2 | 12.1 | MISTRA90 | N90 |
| Superstitt Hills | 1987 | 6.7 | Westmorland Fire Sta | 13.1 | WSM180 | N180 |
| Loma Prieta | 1989 | 6.9 | Gilroy Array #3 | 14.0 | SEWAGE90 | N90 |
| Loma Prieta | 1989 | 6.9 | Gilroy Array #4 | 15.8 | YSIDRO90 | N90 |
| Loma Prieta | 1989 | 6.9 | Gilroy - Historic Bldg. | 16.0 | HIST90 | N90 |
| Superstitt Hills | 1987 | 6.7 | El Centro Imp. Co. Cent | 18.2 | ICC000 | N00 |

Even though they belong to a relatively narrow bin they show some dispersion in frequency content, that is reflected especially in the input energy spectra or pseudo-velocity spectra. As shown in Table 5, the 10

records have comparable values of peak ground velocity (PGV) and Housner Intensity (I_H), while some differences occur for the peak ground acceleration (PGA), the maximum spectral acceleration ($S_{a,max}$) and the effective peak acceleration (EPA). The dispersion in the elastic energy parameter, namely maximum input energy ($E_{I,max}$), and the area enclosed by the input energy spectrum in the period range 0-2 s and 0-4 s ($AE_{I(0-2)}$ and $AE_{I(0-4)}$, respectively, Decanini [19]) is larger.

Table 5. Characteristic parameters of the damage potential of the recorded ground motion

| Station | PGA (cm/s^2) | PGV (cm/s) | $S_{a,max}$ (g) | EPA (g) | I_H (cm) | $AE_{I(0-2)}$ (cm^2/s) | $AE_{I(0-4)}$ (cm^2/s) | $E_{I,max}$ (cm^2/s^2) |
|----------|----------------------------|--------------------------|--------------------|------------|---------------|---|---|---|
| ULCHOLNS | 288 | 39 | 0.844 | 0.247 | 159 | 18808 | 24531 | 32382 |
| KEYSTN14 | 309 | 31 | 0.936 | 0.307 | 124 | 6003 | 11571 | 5470 |
| LOS270 | 473 | 45 | 1.466 | 0.444 | 158 | 13673 | 16858 | 25572 |
| PETROVNS | 445 | 39 | 1.802 | 0.454 | 150 | 22244 | 24478 | 47856 |
| MISTRA90 | 316 | 39 | 1.238 | 0.324 | 185 | 16462 | 19944 | 24530 |
| WSM180 | 207 | 31 | 0.831 | 0.231 | 138 | 11313 | 19499 | 17357 |
| SEWAGE90 | 362 | 44 | 1.395 | 0.332 | 166 | 10373 | 18080 | 10341 |
| YSIDRO90 | 210 | 38 | 1.045 | 0.221 | 132 | 10488 | 13713 | 12870 |
| HIST90 | 280 | 43 | 0.953 | 0.246 | 145 | 9208 | 11725 | 11579 |
| ICC000 | 351 | 46 | 0.921 | 0.262 | 138 | 8128 | 14218 | 6117 |

RESULTS OF THE ANALYSES

As it is well recognized, the addition of infill walls in a reinforced concrete frame structures leads to a decrease of the natural period of the building. From the values of the fundamental periods of the infilled frame structures, illustrated in Table 6, which was estimated in post-cracking conditions, it is clear that the period of the bare frame is on average 2.1, 2.6, 3.5 greater than those of the frames with infills t1, t2, and t3, respectively. These increases in stiffness may cause an increase or decrease of the base shear, depending on both the frame analyzed and the characteristics of the ground motion. For the tall frames, the addition of the infills decreases the corresponding periods which can produce an increase in the strength demand. In the case of short to mid-rise frames, their fundamental periods can move towards the plateau region or the increasing branch of the pseudo-acceleration spectrum. However, these conclusions depend strongly on the characteristics of the motion considered, and on the fact that a large part of the seismic forces can be carried by the infill walls.

Table 6. First mode periods of bare and infilled frames

| N. of stories | T (s) infilled t1 | T (s) infilled t2 | T (s) infilled t3 | T (s) bare frames |
|---------------|-------------------|-------------------|-------------------|-------------------|
| 2 | 0.148 | 0.117 | 0.088 | 0.286 |
| 4 | 0.266 | 0.218 | 0.168 | 0.536 |
| 6 | 0.366 | 0.298 | 0.227 | 0.761 |
| 8 | 0.479 | 0.389 | 0.296 | 1.015 |
| 10 | 0.581 | 0.470 | 0.356 | 1.251 |
| 12 | 0.674 | 0.544 | 0.411 | 1.465 |
| 14 | 0.764 | 0.616 | 0.465 | 1.664 |
| 16 | 0.862 | 0.695 | 0.523 | 1.874 |
| 20 | 1.048 | 0.841 | 0.630 | 2.338 |
| 24 | 1.209 | 0.970 | 0.725 | 2.689 |

As far as the top displacement, δ_{top} , is concerned, the presence of infill walls always entails a decrease in such parameter, as natural consequence of the stiffening of the structure. Figure 5 illustrates the mean trend of the top displacement over the various signal considered, a function of the number of storeys, N, for $C_y=0.15$ and $C_y=0.40$. As it can be observed, while the influence of the coefficient C_y is negligible, the

addition of infill walls gradually stiffer and more resistant appears to produce a considerable decrease in the value of top displacement.

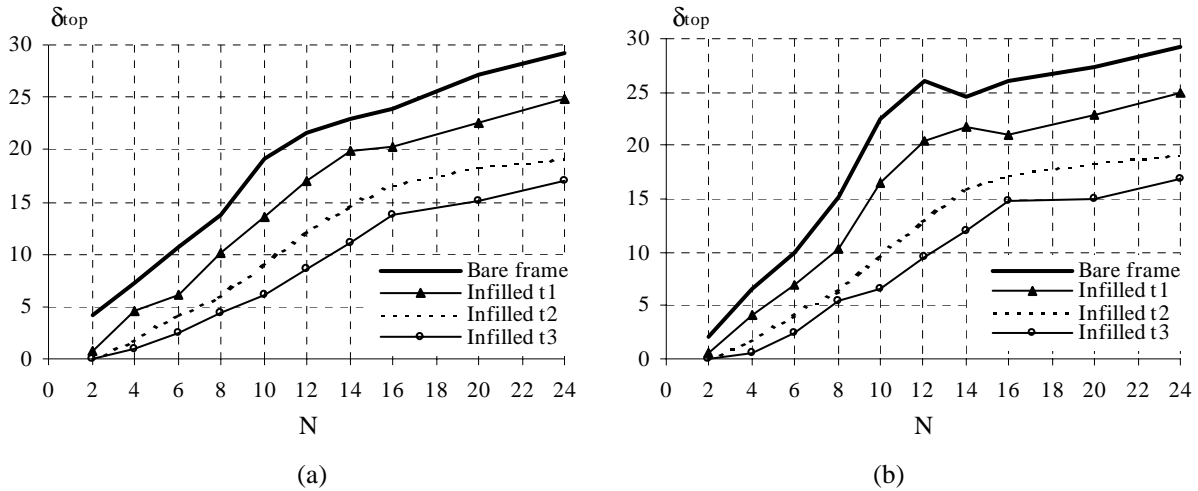


Figure 5. Top displacement, δ_{top} , vs. number of storeys, N. Mean values. (a) $C_y=0.15$; (b) $C_y=0.40$

An interesting aspect is connected with the comparison of the conventional displacement spectra for single-degree-of-freedom (SDOF) systems and the top displacement spectra, corresponding to a seismic coefficient $C_y=0.15$, evaluated for the bare and infilled frames (Figure 6).

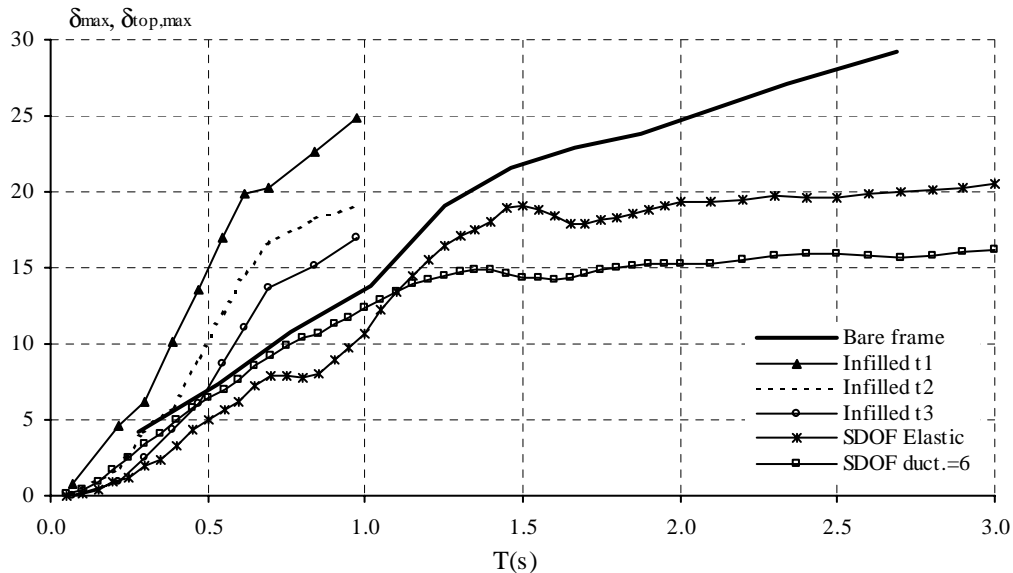


Figure 6. SDOF elastic and inelastic (ductility ratio equal to 6) displacement, δ_{max} , spectra vs. maximum top displacement, $\delta_{top,max}$, spectra of bare and infilled frames ($C_y=0.15$)

It can clearly be detected that the spectrum relevant to the bare frames does not diverge significantly from the elastic and inelastic (ductility ratio equal to 6) relevant to the SDOF systems, at least for periods less than 1.5 s; greater differences being evident with relevance to tall frames (i.e., for $T>1.5$ s), as a consequence of the amplification effect due to the upper vibration modes. On the contrary, spectra relevant to the infilled frames all appear shifted towards the high frequency region, thus exhibiting maximum displacements greater than those evaluated for SDOF systems. In conclusion, as expected, conventional displacement spectra for SDOF systems can not be considered representative of the actual

displacement demands for infilled frames. Such spectra need to be modified in order to take into account the stiffening of the infilled frames to the respect of the bare frames.

Figure 7 illustrates the mean values of the maximum inter-story drift index, IDI_{max} , over ten different ground motions as a function of the number of stories, N , for bare and infilled t1 frames and four values of the seismic coefficient, C_y . It was found that the influence of C_y is significant for the lowest frames, from 2 to 8 stories for the bare frames, and from 2 to 12 stories for the infilled t1, t2 and t3 frames.

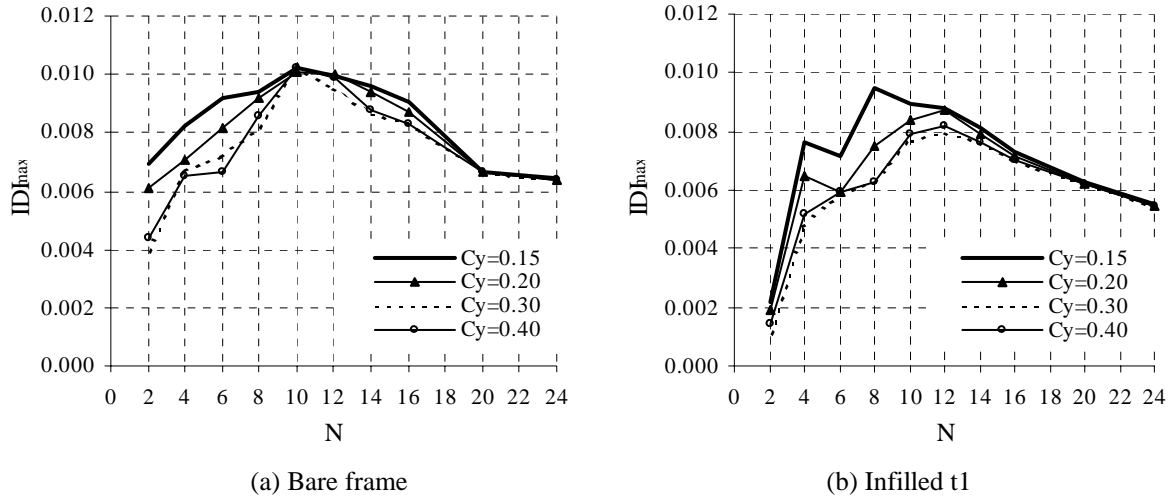
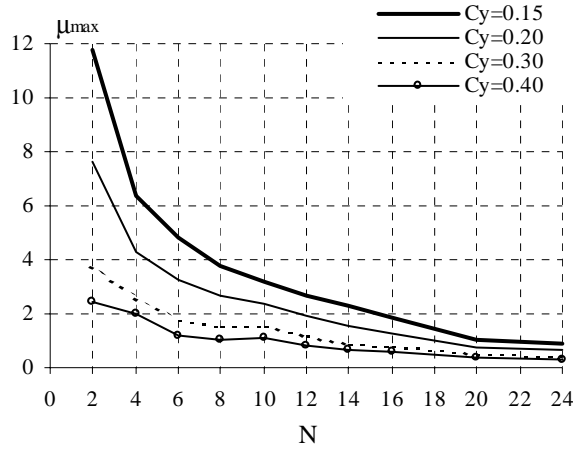


Figure 7. Maximum inter-story drift, IDI_{max} vs. n. of storeys, N . Mean values. Influence of the coefficient C_y .

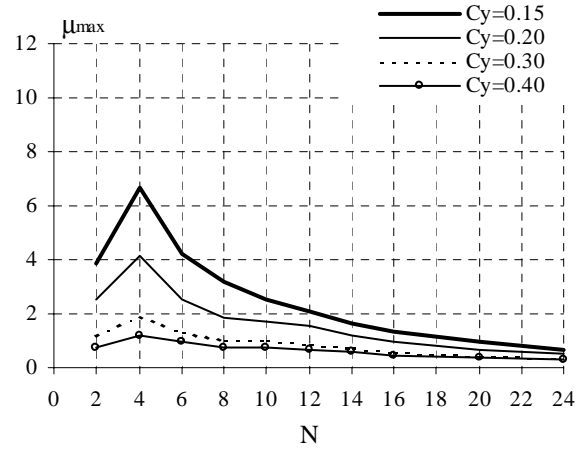
This behaviour can be better understood by comparing the response of the frames in terms of the maximum storey ductility demand, μ_{max} . The story ductility demand over the height constitutes a measure of the degree of inelastic behaviour experienced by the MDOF systems. As it can be observed in Figure 8a for the bare frame a large μ_{max} occurs in the lowest frames with large differences as a function of the number of storeys and the C_y coefficients. Such ductility demand tends to decrease significantly in the infilled frames. As in the case of bare frames, the largest values of μ_{max} are attained by the lowest frames; moreover, further decreases in the maximum ductility occur as a function of the mechanical characteristics of the infill walls, from t1 to t3 (Figures 8 b, c, d). It is also worth noting that, for a fixed number of storeys, N , the maximum ductility demand tends to concentrate towards the lowest storeys of the infilled frames. It should be considered that, while in the bare frames the dissipated energy demand tends to increase significantly as the coefficient C_y decreases, in the infilled frames the dissipated energy demand does not appear to be appreciably affected by a variation in the value of the seismic coefficient.

Furthermore, while the energy dissipated in the bare frames tends to decrease as the number of storeys increases, until an elastic behaviour is achieved, in the infilled frames an increasing in the energy dissipation with the number of storeys always occurs. In comparison with the great amount of dissipated energy in the medium-to-long period range in presence of infill walls, the response of the bare frames does not develop in the inelastic range significantly. In fact, for $C_y=0.15$ the maximum story ductility for $N > 12$ does not attain values greater than 2.5, which corresponds to a mean global ductility not exceeding 1.2-1.3. Such circumstances imply that an approximately elastic response, i.e. the one relevant to the bare frames, is compared with a response characterized by the markedly inelastic behaviour of the infill walls.

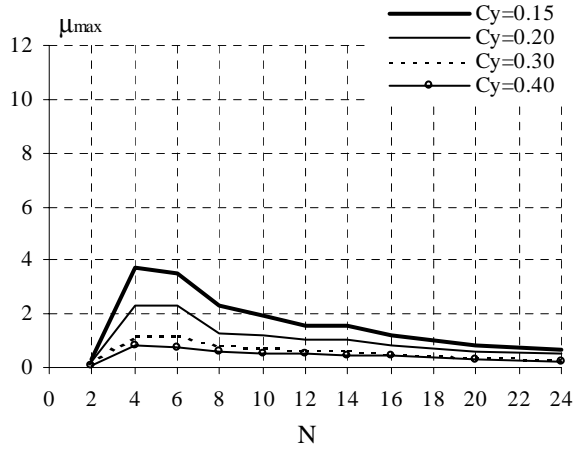
However, the story ductility demand in the infilled frames designed according to current design guidelines experienced a highly non-uniform distribution as it tends to concentrate in a few stories.



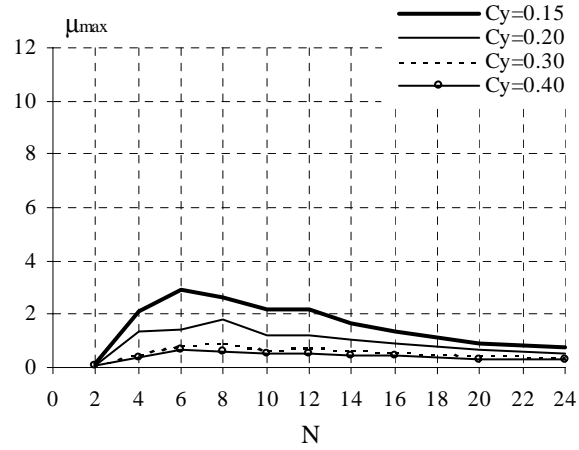
(a) Bare frame



(b) Infilled t1



(c) Infilled t2

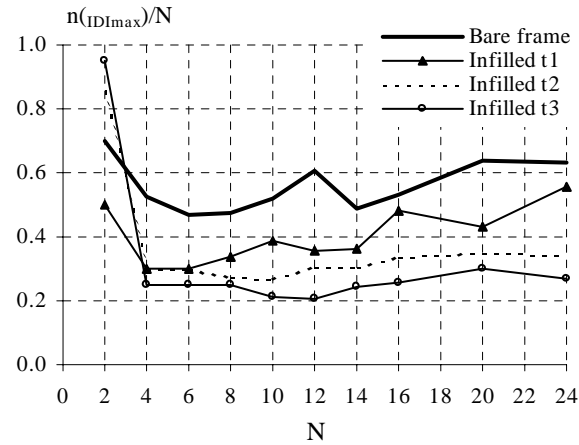


(d) Infilled t3

Figure 8. Maximum ductility demand, μ_{max} vs. n. of storeys, N . Mean values. Influence of the coefficient C_y .



(a) IDI_{max} vs. number of storeys, N



(b) $n(IDI_{max})/N$ vs. number of storeys, N

Figure 9. (a) Mean demands of IDI_{max} and $n(IDI_{max})/N$. Influence of the infills. $C_y=0.15$

Comparing, the mean trends of the maximum inter-story drift, IDI_{max} , as a function of the number of storeys (Figure 9a, for $C_y=0.15$), the beneficial effects of the presence of infill walls on the reduction of the relative story displacement can be appreciated. Such effects are particularly marked with relevance to the masonry infills characterized by high values of the maximum strength, infill wall type t2 especially. Furthermore, from Figure 9b, with $n(IDI_{max})$ representing the story where the maximum value of the drift is attained, a shift of the maximum drift demand in the infilled towards the lowest storeys is clearly detectable. Actually, it can also be observed that the drift demand for frames with infill type t3 is greater than relevant to frames with infill type t2, and tends to approach the spectrum evaluated for frames with infill type t1 as soon as $N>10$ storeys. Such behaviour, often detected in tall frames also through analyses performed at constant ductility ratios (Mura [12]), can be related with local ruptures in the masonry, whose brittle behaviour implies the sudden loss of the associated contribution to the storey strength and stiffness, with consequent local concentration of the drift demand and a sharp variation of the resistance over the height. Such phenomenon is amplified in presence of infill type t3, for which the hysteretic envelope is characterized by a softening branch whose slope is about twice as much as that of infill type t2. Moreover, the degrading effect in infill type t3 due to the energy dissipation, measured by the factor β , which also is for t3 twice as much as for t2, is considerably more rapid than in infill type t2. The consequence is that the masonry infill t3 is more brittle and thus more affected by a cyclic degradation. The knowledge of the distribution of the inter-story drifts over the height provides additional information in gaining a better understanding of the different behaviour of bare and infilled frames. A graphical representation of the distribution of the mean values of the IDI_{max} along the height of structures with 4, 8 and 12 stories are given in Figures 10 and 11 for $C_y=0.15$ and $C_y=0.40$, respectively. The 4 story bare frames exhibit an approximately uniform distribution of maximum inter-story drift demands, while for the 8 and 12 story frames the distribution of inter-story drifts over the height tends to concentrate at the upper portions of the frames. In the case of infilled frames, the maximum inter-story drift demand migrates from the top stories to the bottom ones. This effect is more evident as the stiffness and strength of infills are increased starting from t1 to t2 and t3 types. Moreover, the quantity IDI_{max} is also amplified at the bottom stories of the infilled frames, particularly for a high degree of inelastic behaviour experienced by the masonry infills as it happens for $C_y=0.15$.

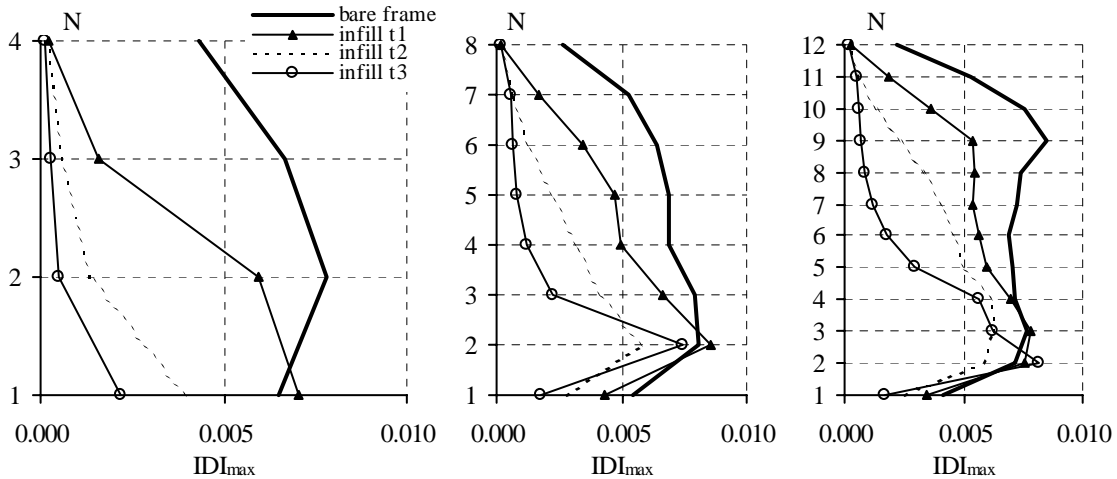


Figure 10. IDI_{max} demands along the height of bare and infilled frames. $N=4, 8, 12$. Mean values. $C_y=0.15$

However, the way in which the structural behaviour is modified by the addition of the infills not only is connected with the height of the frames, but also depends on the considered ground motions. In fact, even though the selected ground motions belong to a narrow magnitude and distance range and to a specific soil class, in some cases there is some variation in the frequency content and in the amplitude, which

could lead to a significant dispersion in the response of the infilled frames, particularly in highly inelastic systems.

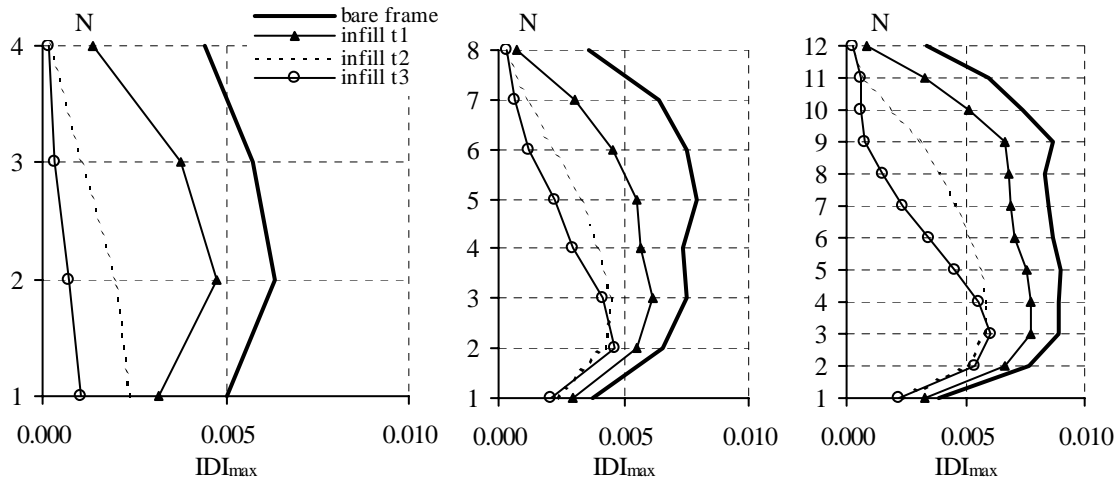


Figure 11. IDI_{max} demands along the height of bare and infilled frames. $N=4, 8, 12$. Mean values. $C_y=0.40$

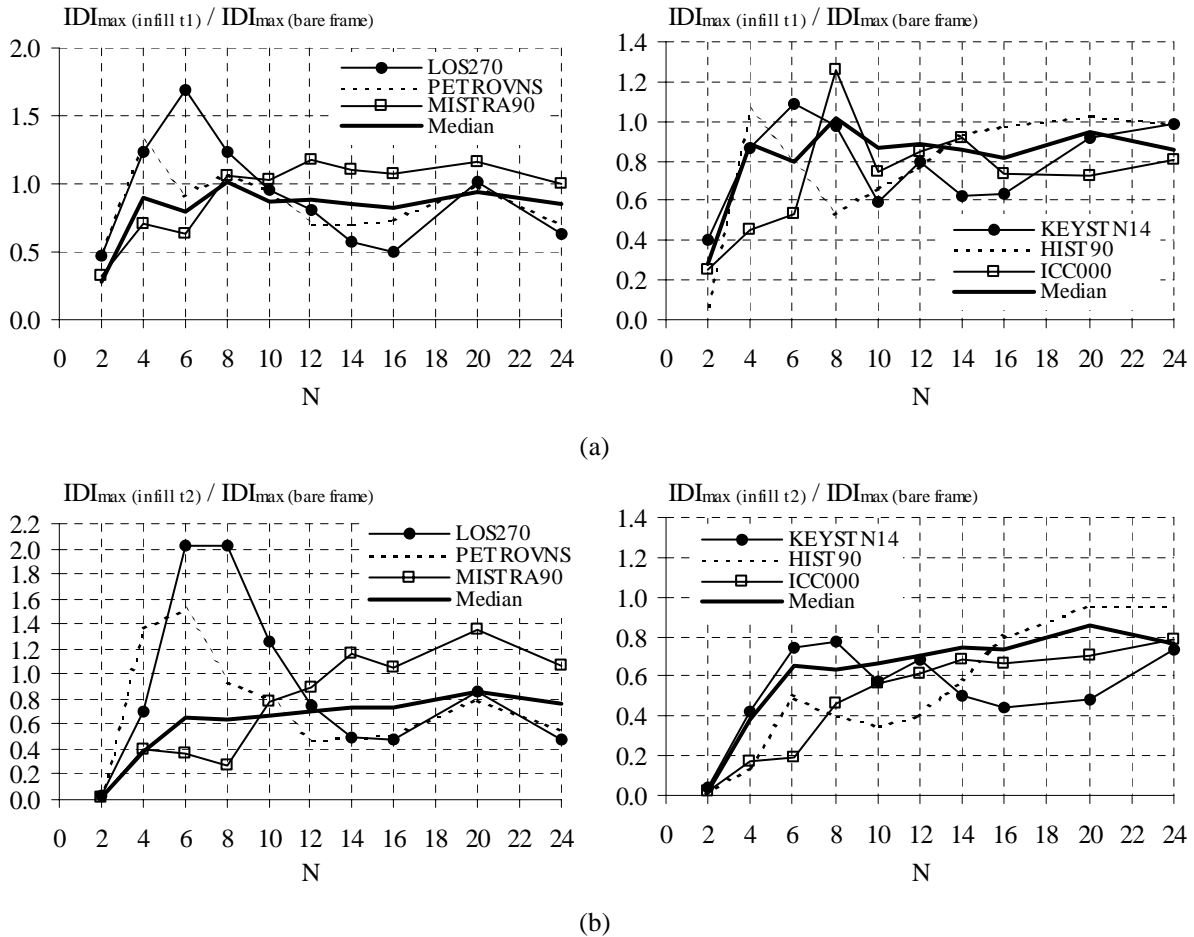


Figure 12. Ratio of the maximum inter-story drift for the infilled frame to that relevant to the bare frame. $C_y=0.15$. (a) IDI_{max} (infilled t1) / IDI_{max} (bare frame); (b) IDI_{max} (infilled t2) / IDI_{max} (bare frame).

To this purpose two groups of three ground motions each were selected in order to highlight the variation of the response in terms of IDI_{max} for the infilled frames. The former contains the signals denoted as LOS270, PETROVNS and MISTRA90, while the latter encloses the signals denoted as KEYSTN14, HIST90 and ICC000. Such a choice permitted to reduce considerably the coefficient of variation of the various parameters considered in Table 5.

In Figure 12 the ratio of the maximum inter-story drift for the infilled frame to that relevant to the bare frame is illustrated for infill types t1 and t2, and for the two groups of signals listed above. As far as the first group is concerned, the maximum difference from the median trend is observed particularly for the LOS270 and PETROVNS records for N varying from 4 to 8 storeys. Regarding the second group of signals, as a general rule the maximum demand of inter-story drift for the infilled frames is less than that relevant to the bare frames. It can be noted that LOS270 and PETROVNS determine the maximum strength demand in terms of PGA, S_{amax} and EPA (Table **). Such demand may cause at the bottom storeys of the infilled frames a large deformation demand which could exceed the drift capacity leading to the development of a soft-storey mechanism.

CONCLUSIONS

In this paper the influence of masonry infills on the seismic performance reinforced concrete frames was investigated. The infill panels, modelled with equivalent strut elements carrying only compressive loads, were implemented in a simplified shear-type model in order to obtain also a spectral representation of the seismic demands of the frame structures systems at global and local level. Three type of masonry infills, classified as weak (t1), intermediate (t2), and strong (t3), were considered in the analyses. It was found that the presence of infill walls, gradually stiffer and more resistant, results in a significant decrease in the value of top displacement, as natural consequence of the stiffening of the structure. It was found that the influence of C_y is significant for the lowest frames, from 2 to 8 stories for the bare frames, and from 2 to 12 stories for the infilled t1, t2 and t3 frames.

The story ductility demand over the height, which constitutes a measure of the degree of inelastic behaviour experienced by the MDOF systems, tends to decrease significantly in the infilled frames and to concentrate towards their lowest storeys with respect to the bare frames. Further decreases in the maximum ductility occur as a function of the mechanical characteristics of the infill walls, from t1 to t3. Moreover, it must be noted that, even for low values of the story ductility demand, the infilled frames may experience a markedly inelastic behaviour with a highly non-uniform distribution as it tends to concentrate in a few stories. This effect causes also a shift of the maximum drift demand in the infilled frames towards the lowest storeys that can result in the development of a soft-storey mechanism. Such a behaviour was also sometimes detected for the infill type t3, that, even more resistant than the infill type t2, is more brittle and more affected to a cyclic degradation. However, it must be noted that in almost all cases the contribution of the infills to the increase of the dissipation capacity of the frames is significant and not much affected by the resistant capacity of the bare frame. These conclusions depend strongly on the characteristics of the motion considered, even though the selected ground motions for a specific soil class belong to a narrow magnitude and distance bins. In fact, in some cases a significant dispersion in the response of the infilled frames, particularly in high inelastic systems, was detected.

Finally, the performance of the infilled frames, for a given type of infills, can be improved increasing the strength capacity of the bare frame rather than increasing its ductility capacity, as far as for limited ductility demand the infills may undergo to significant inelastic deformation demands.

ACKNOWLEDGEMENTS

The financial support of the Ministry of the Instruction, University and Research of Italy (MIUR) is gratefully acknowledged.

REFERENCES

1. Crisafulli, F. J., Carr, A. J., and Park, R., (2000), "Analytical Modeling of Infilled Frame Structures - A General Review", Bulletin of the New Zealand Society for Earthquake Engineering, Vol. 33, No. 1, pp 30-47.
2. Shing P. B., Mehrabi A.B., (2002) "Behaviour and analysis of masonry-infilled frames", Prog. Struct. Engng Mater. 2002; 4, 320-331.
3. Klingner R.E., Bertero V.V. (1978) "Earthquake resistance of infilled frames", Journal of Structural Engineering, ASCE, 104(ST6): 973-989.
4. Bertero, V.V., Brokken S.T., (1983). "Infills in seismic resistant buildings", Journal of Structural Engineering, ASCE, 109(6): 1337-1361.
5. Decanini, L.D., Bertoldi, S.H., Gavarini, C., (1993), "Telai tamponati soggetti ad azioni sismiche, un modello semplificato, confronto sperimentale e numerico", Atti del 6° Convegno Nazionale L'ingegneria Sismica in Italia, Perugia, 13-15 Ottobre 1993, 2, 815-824 (in Italian).
6. Kappos, A. J., Stylianidis, K. C. and Michailidis, C. N., (1998), "Analytical models for brick masonry infilled R/C frames under lateral loading", Journal of Earthquake Engineering, Vol. 2, No.1, 59-87.
7. Fardis, M.N. & Panagiotakos T.B. (1997), "Seismic design and response of bare and infilled reinforced concrete buildings. Part II: Infilled structures", J. Earthq. Engrg., IC Press, 1(3):475-503.
8. Decanini L, Mollaioli F, Mura A. (2004) "Simplified shear-type model for the evaluation of the influence of ductility and stiffness distribution patterns on multi-story structures", XI Italian National Conference "L'ingegneria Sismica in Italia", Genova, Italy, January 25-29, 2004.
9. Decanini L.D., Fantin G.E., (1986), "Modelos simplificados de la mamposteria incluida en porticos. Caracteristicas de rigidez y resistencia lateral en estado limite", Jornadas Argentinas de Ingenieria Estructural, Buenos Aires, Argentina, 1986, Vol.2, pp.817-836 (in Spanish).
10. Decanini, L., Gavarini C., Mollaioli F., Bertoldi S.H., (1994), "Modelo simplificado de paneles de mamposteria con aberturas incluidos en marcos de concreto reforzado y metalicos. comparacion y calibracion con resultados experimentales y numericos". 9th International Seminar on Earthquake Prognostics, San José, Costa Rica, 19-23 September 1994 (in Spanish).
11. Stafford Smith, B., (1963), "Lateral stiffness of infilled frames", Journal of Structural Division, ASCE, Vol. 88, No. ST 6, pp 183-199.
12. Mura A. (2003) "Sulla valutazione del potenziale di danno in termini di spostamenti e di energia sui sistemi a più gradi di libertà soggetti ad eccitazione sismica", Ph.D. Dissertation Thesis, Department of Structural and Geotechnical Engineering, University of Rome "La Sapienza", Italy (in Italian).
13. Liberatore, L., (2001), "Approcci innovativi in termini di energia e di spostamento per la valutazione della risposta sismica di strutture a più gradi di libertà", PhD Dissertation Thesis, Department of Structural and Geotechnical Engineering, University of Rome "La Sapienza", Italy (in Italian).
14. Parducci, A. & Mezzi, M., (1980), "Repeated horizontal displacements of infilled frames having different stiffness and connection systems – experimental analysis". Proceedings of The Seventh World Conference on Earthquake engineering. Istanbul, Turkey.
15. Parducci, A. & Checchi, A., (1982) "Contributo delle tamponature di mattoni alla resistenza sismica delle strutture intelaiate", Proceedings of Sixth International Brick Masonry Conference. Roma.
16. Stylianidis, K. C., (1988), "Cyclic Behaviour of infilled R/C frames", Proceedings of 8th Conference IBMaC. Dublin.
17. Pires, F. M., (1990), "Influência das paredes de alvenaria no comportamento de estruturas reticuladas de betão armado sujeitas a ações horizontais", PhD Dissertation. Laboratorio Nacional de Engenharia Civil. Lisboa.
18. EC8 (Eurocode 8), European Standard Design of structures for earthquake resistance, prDRAFT no.3, May 2001.
19. Decanini L, Mollaioli F. (1998) "Formulation of elastic earthquake input energy spectra". Earthquake Engineering and Structural Dynamics, 27, 1503-1522.